Supplementary Information for:

Photoelectrochemical Behavior of n-Type GaAs(100) Electrodes Coated by a Single Layer of Graphene

*Fan Yang, Adam C. Nielander, Ronald L. Grimm# and Nathan S. Lewis**

Division of Chemistry and Chemical Engineering, California Institute of Technology, Pasadena, CA, 91125, United States

Correspondence to: nslewis@caltech.edu

Experimental Methods

Materials and Chemicals

A series of redox couples that have an effective potential ranging from -0.87 V to 0.23 V vs the saturated calomel electrode (SCE) was used in the electrochemical studies. The preparation and purification of chemicals were exactly the same as reported previously.[1] The iron complexes, decamethylferrocene (Cp^*_2Fe, bis(pentamethylcyclopentadienyl)iron, 99%, Strem), octamethylferrocene (Me_8Cp_2Fe, bis(tetramethylcyclopentadienyl)iron, 98%, Strem), 1,1′-dimethylferrocene (Me_2Cp_2Fe, bis(methylcyclopentadienyl)iron, 95%, Sigma-Aldrich) and ferrocene (Fc, bis(cyclopentadienyl)iron(II) ,99%,Strem) were purified via sublimation. The salts decamethylferrocenium ($Cp^*_2Fe^+BF_4^-$, bis(pentamethylcyclopentadienyl)ferrocenium tetrafluoroborate), octamethylferrocenium ($Me_8Cp_2Fe^+BF_4^-$, bis(tetramethylcyclopentadienyl)-ferrocenium tetrafluoroborate), and 1,1′-dimethylferrocenium ($Me_2Cp_2Fe^+BF_4^-$, bis(methylcyclopentadienyl)ferrocenium tetrafluoroborate) were synthesized by chemical oxidation of the

neutral metallocenes[2]. Ferrocenium tetrafluoroborate ($Cp_2Fe^+BF_4^-$, bis(cyclopentadienyl)-iron(III) tetrafluoroborate, technical grade, Sigma-Aldrich) was purified by recrystallization. Cobaltocene (Cp_2Co, bis(cyclopentadienyl)cobalt(II), 98%, Strem) was purified by vacuum sublimation, whereas cobaltocenium ($Cp_2Co^+PF_6^-$, bis(cyclopentadienyl)cobaltocenium hexafluorophosphate, 98%, Sigma-Aldrich) was recrystallized from an ethanol (ACS grade, EMD)/acetonitrile (ACS grade, EMD) mixture and was dried under vacuum. Both 1,1′-dicarbomethoxycobaltocene ($(CpCO_2CH_3)_2Co$, 1,1′-bis(η^5-methoxycarbonylcyclopentadienyl)-cobalt) and the oxidized $(CpCO_2CH_3)_2Co^+$ species were synthesized by reacting $CoCl_2$ with the lithium reagent of the functionalized cyclopentadienyl moiety.[3-4] For the nickel-containing compounds, octamethylnickelocene (Me_8Cp_2Ni, bis(tetramethylcyclopentadienyl)nickel, 98%, Strem) was purified by sublimation. Octamethylnickelocenium ($Me_8Cp_2Ni^+BF_4^-$, bis(tetramethylcyclopentadienyl)nickelocenium tetrafluoroborate) was synthesized by the chemical oxidation of octamethylnickelocene, and was purified by recrystallization.[2]

Calculation of the effective solution potential $E_{eff}(A/A^-)$

The calculation of the effective solution potential was performed using a previously published procedure.[1] Effective solution potentials, $E_{eff}(A/A^-)$, were calculated based on $E(A/A^-)$ and the concentrations of the redox species. The concentration correction for the A/A^- redox species performed in this study followed conditions previously reported.[5] Figure S1 shows the effect of this concentration correction for an n-type semiconductor-liquid junction photoelectrochemical cell. Point A denotes a V_{oc} that was experimentally measured in a solution with redox potential $E(A/A^-)$ at which the concentration of oxidized species [A] and reduced species [A^-] are not at ideal values for comparison to other photoelectrochemical V_{oc} vs $E(A/A^-)$ values. In

order to normalize to a consistent minority-carrier acceptor concentration, we consider a dilution of the redox species concentration ratio to $[A]'$ and $[A^-]'$, in which $[A]'$ =c[A] and $[A^-]'$=c$[A^-]$. This uniform change does not change the Nernstian solution potential, but will introduce a change on the V_{oc} for ideally behaving systems over a certain range. Equation S1 describes this change for n-type semiconductor-liquid junctions,

$$V'_{oc,n} = V_{oc,n} + \frac{k_B T}{q} \ln \frac{[A^-]}{[A^-]'} \quad \text{(S1)}$$

In equation S1, k_B is the Boltzmann's constant, T is the temperature, and q is the fundamental unit of charge. In the case of $[A^-]' > [A^-]$, V_{oc} decreases from point A in Figure S1 to point B, while $E(A/A^-)$ remains unchanged. This open-circuit photovoltage, V_{oc}', represents the value that would be obtained if the photoelectrochemical cell contained redox species in concentrations $[A]'$ and $[A^-]'$.

Equation S2 describes the linear change in V_{oc} between two electrochemical cells with redox couples A/A^- and B/B^- when [A]=[B] and $[A^-]$=$[B^-]$ for n-type semiconductor-liquid junctions.

$$V_{oc,n,b} = V_{oc,n,a} + E(B/B^-) - E(A/A^-) \quad \text{(S2)}$$

The shift from point B to point C in Figure S1 represents the change in V_{oc} at an n-type semiconductor accompanied by a shift in solution potential from $E(A/A^-)$ to $E(B/B^-)$ when $[A]'$=[B] and $[A^-]'$=$[B^-]$. Thus, the overall shift from point A to point C represents the shift to the effective solution potential, $E_{eff}(A/A^-)$, which is needed for the comparison of V_{oc} vs $E(A/A^-)$ relationships that have been determined by measurement using different redox species at mutually different concentrations.

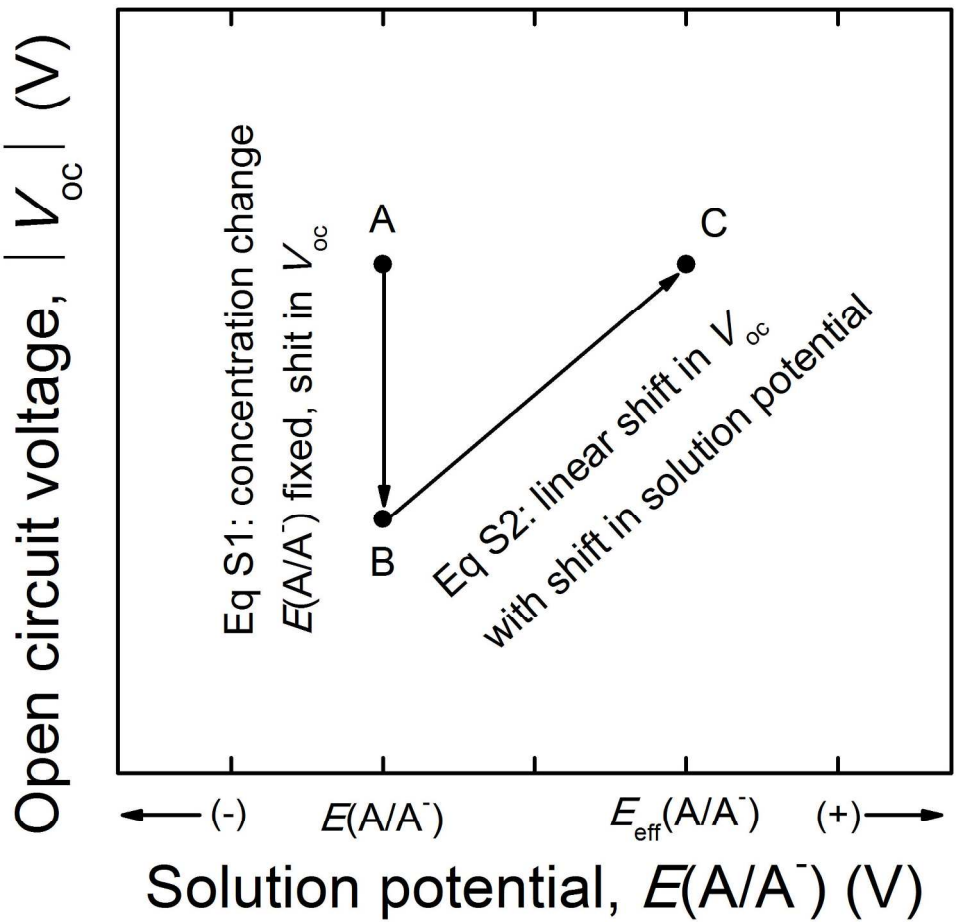

Figure S1. Schematic graph replotted from previous report[1] to illustrate the shift from experimental solution potential $E(A/A^-)$ to an effective potential $E_{eff}(A/A^-)$ for comparison of V_{oc} vs $E(A/A^-)$.

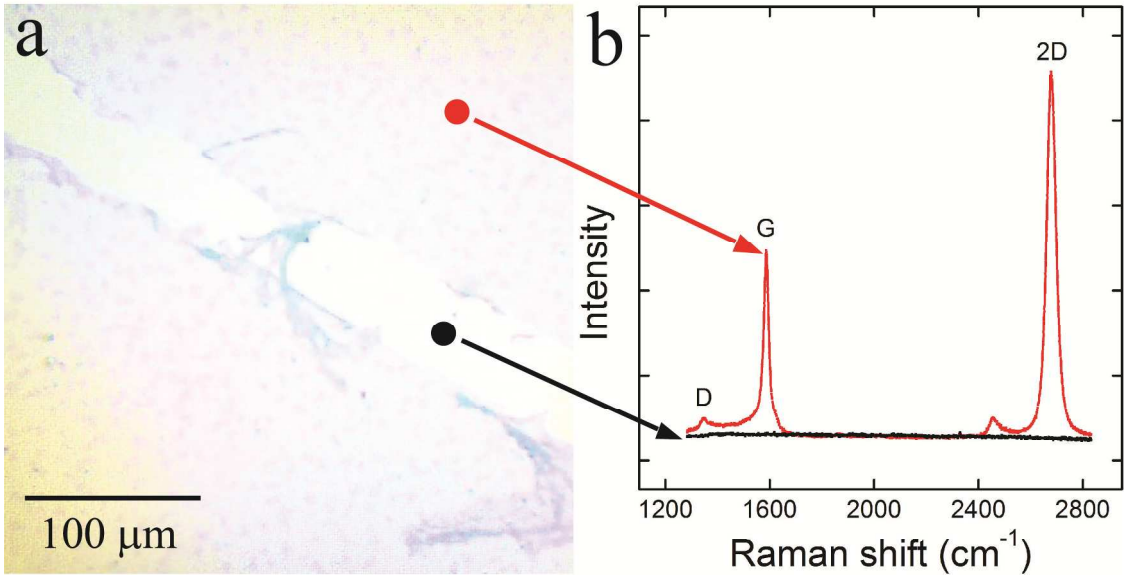

Figure S2. (a) Optical image of single graphene layer on 300 nm SiO_2. (b) Raman spectroscopy from monolayer graphene (red curve) and background SiO_2 (black curve).

The electrochemical impedance data were fit to a Randles circuit model that consisted of a parallel resistor and capacitor arranged electrically in series with a separate resistor (Figure S3). Analysis of the impedance data was performed using a custom LabVIEW program. Data were fit in the frequency range between 10^3 and 10^5 Hz, in which the parallel capacitance dominates. The differential capacitance C_{diff} is approximated to the space-charge capacitance C_{sc} of the semiconductor and was employed to calculate the flat-band potential, E_{fb}, through the Mott–Schottky relationship, eq S3:

$$A^2 C_{diff}^{-2} = \frac{2}{q\epsilon\epsilon_0 N_d}(E - E_{fb} - \frac{k_B T}{q}) \quad \text{(S3)}$$

In eq S3, A is the area of the semiconductor-liquid junction, ϵ is the dielectric constant of GaAs, ϵ_0 is the permittivity of vacuum, N_{d} is the doping density of the sample, T is the absolute temperature, k_{B} is Boltzmann's constant, and q is the (unsigned) charge on an electron.

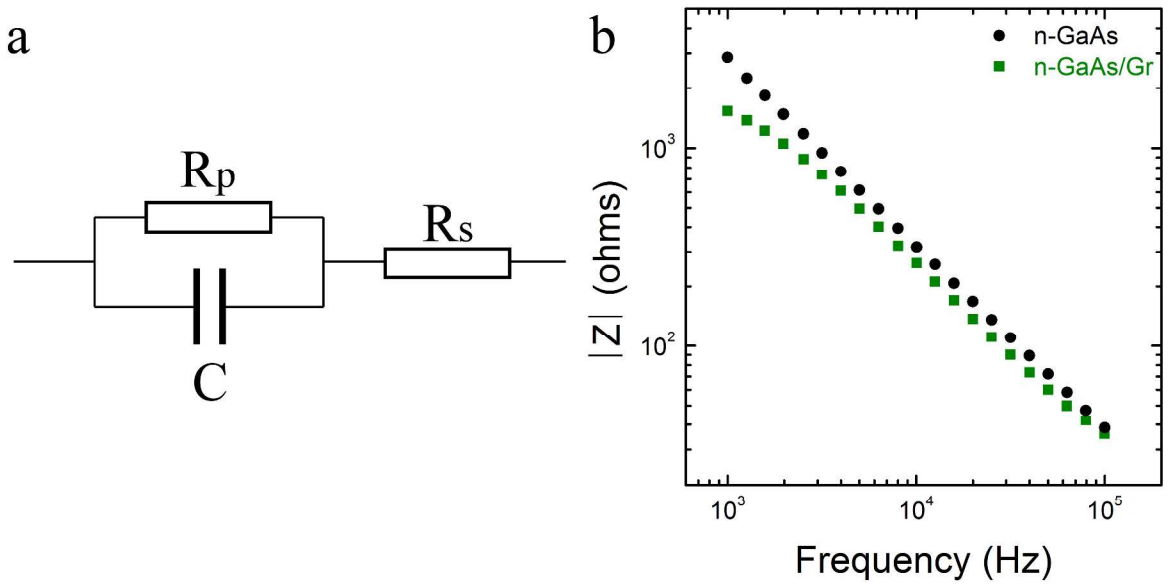

Figure S3. (a) Randles circuit for modeling the impedance data. (b) Bode plot of n-GaAs (black circle) and n-GaAs/Gr (olive square) electrodes in contact with CH_3CN-$Fc^{+/0}$ in the absence of illumination at E = 0.40 V vs. the Nernst potential of the solution.

The presence of graphene has been predicted[6] to reduce the portion of the potential drop across the GaAs/Gr/electrolyte interface that occurs within the space-charge region of the GaAs relative to the potential drop attributable to the GaAs space-charge region for the equivalent graphene-free GaAs/electrolyte interface. The Randles circuit model used in this work to fit the electrochemical impedance data for this work does not account for the potential drop across the graphene and Helmholtz layers. However, the model can be used to calculate the correct flat-band potential, V_{fb}, because the capacitances due to any potential drops across the graphene or Helmholtz layers are in series with the space-charge capacitance and are much larger than the space-charge capacitance. The capacitance due to any potential drops across the graphene or Helmholtz layers is thus a very small fraction of the total differential capacitance of the system, because the capacitance of two capacitors in series is dominated by the smallest capacitor. Rela-

tive to the actual behavior of the system, the Randles circuit model will however produce a larger change in potential drop for a given change in potential applied to the space-charge layer. The use of this model therefor results in an overestimation of the capacitance of the space-charge layer. Because the measured capacitance varies less as a function of applied potential than predicted, the slope of a linear plot of $1/C_{\mathrm{diff}}^{2}$ vs. E is reduced relative to the value when the graphene is absent, thereby resulting in an overestimation of the dopant density for the GaAs/Gr/electrolyte case.

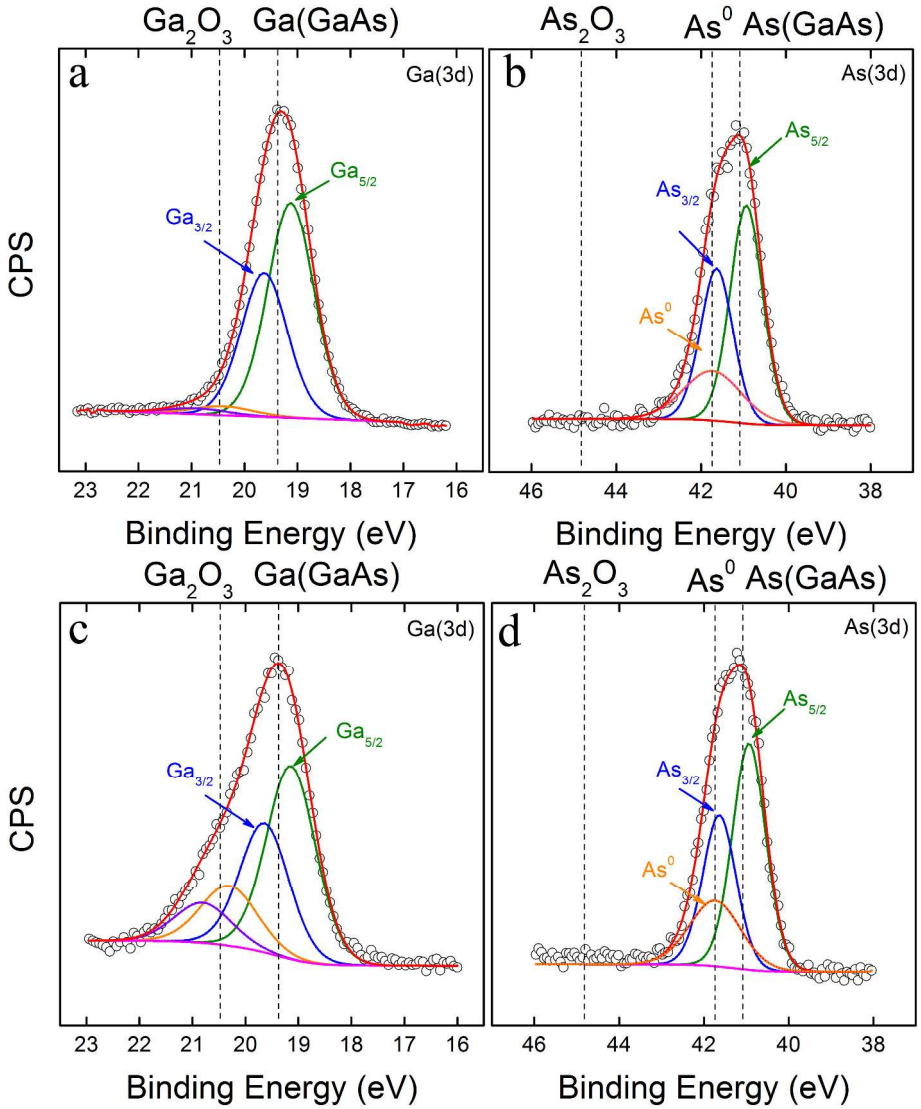

Figure S4. Representative high-resolution XP spectrum of (a) Ga 3d and (b) As 3d region of a freshly etched GaAs in comparison with (c) Ga 3d and (d) As 3d of a graphene-covered GaAs wafer.

XPS analysis was performed on an M-Probe spectrometer with a base pressure of $< 1 \times 10^{-9}$ Torr. All XP spectra were corrected to an adventitious C 1s binding energy peak of 284.6 eV. Data analysis was performed using CasaXPS software (CASA Ltd., Teignmouth, United Kingdom). Freshly etched GaAs was directly vacuum-transferred to the XPS chamber without exposure to air. Analysis of the XPS data of Fig S4a and S4b indicated that only trace amount of oxides were detectable on the surface. The graphene-covered GaAs wafer demonstrated about ~ 1 ML of Ga_2O_3 and trace amounts of As_2O_3 on the surface, as shown in Fig S4c and S4d.

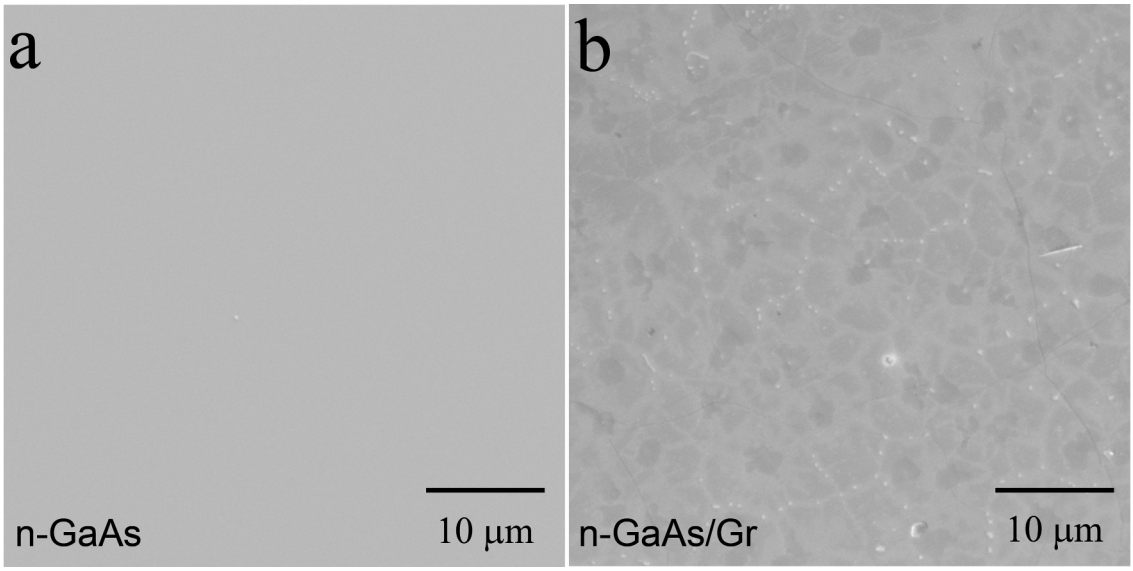

Figure S5. SEM image of (a) freshly etched GaAs and (b) graphene-covered GaAs.

Scanning Electron Microscope images were acquired with a Zeiss 1550VP Field Emission SEM with the in-lens SE mode at high voltage of 15 KV and working distance of 5 mm. The surface morphology of a freshly etched n-GaAs and a graphene-covered GaAs were compared.

Supporting Information References

(1) Grimm, R. L.; Bierman, M. J.; O'Leary, L. E.; Strandwitz, N. C.; Brunschwig, B. S.; Lewis, N. S., Comparison of the Photoelectrochemical Behavior of H-Terminated and Methyl-Terminated Si(111) Surfaces in Contact with a Series of One-Electron, Outer-Sphere Redox Couples in CH_3CN. *J. Phys. Chem. C* **2012**, *116*, 23569-23576.

(2) Gray, H. B.; Hendrickson, D. N.; Sohn, Y. S., Magnetic Susceptibility Study of Various Ferricenium and Iron(III) Dicarbollide Compounds. *Inorg. Chem.* **1971**, *10*, 1559-1563.

(3) Hart, W. P.; Macomber, D. W.; Rausch, M. D., A New, General Route to Functionally Substituted η^5-Cyclopentadienyl Metal Compounds. *J. Am. Chem. Soc.* **1980**, *102*, 1196-1198.

(4) Sheats, J. E.; Rausch, M. D., Synthesis and Properties of Cobalticinium Salts. I. Synthesis of Monosubstituted Cobalticinium Salts. *J. Org. Chem.* **1970**, *35*, 3245-3249.

(5) Rosenbluth, M. L.; Lewis, N. S., "Ideal" Behavior of the Open Circuit Voltage of Semiconductor/Liquid Junctions. *J. Phys. Chem.* **1989**, *93*, 3735-3740.

(6) Nielander, A. C.; Bierman, M. J.; Petrone, N.; Strandwitz, N. C.; Ardo, S.; Yang, F.; Hone, J.; Lewis, N. S., Photoelectrochemical Behavior of N-Type Si(111) Electrodes Coated with a Single Layer of Graphene. *J. Am. Chem. Soc.* **2013**, *135*, 17246-17249.